Synthesis and Characterization of a NLO crystal - bis (thiourea) zinc sulphate doped with L-malic acid

B. Sivasankaria[*1] and P.Selvarajan[2]

1.* Department of physics, The Standard Fireworks Rajaratinam College for women, Sivakasi- 626 123, India; e-mail : sivasankari-physics@sfrcollege.edu.in,

2. Department of Physics, Aditanar Collegeof Arts and Science, Tiruchendur- 628216, India, e-mail : sivasathyan198@gmail.com

Publication Info

Article history :

Received : 22th June, 2019

Accepted : 30th July, 2019

DOI : 10.18090/samriddhi.v11i01.10

Keywords : A1: SHG; B1: force constant; C1:Hardness; D1: NLO.

***Corresponding author :**

B. Sivasankari

e-mail :

sivasankari-physics@sfrcollege.edu.in

Abstract

The nonlinear optical (NLO) material L-malic acid bis(thiourea) zinc sulphate (LMBTZS) was grown by slow evaporation method. The effect of L-malic acid doping on the morphology of the LMBTZS single crystal has been studied. The unit cell parameters were determined by single crystal XRD. The functional groups and force constant of LMBTZS was identified by FTIR analysis. The photoluminescence spectrum of LMBTZS shows the strong emission in ultraviolet region. The thermal behaviours were identified by TG/DTA analyses. Dielectric studies of the grown crystal was carried out. The SHG efficiency was confirmed by powder technique of Kurtz and Perry. LMBTZS is found to be an excellent NLO and piezo-electric material.

1. INTRODUCTION

The semiorganic crystals [1–5] are used as new frequency generators, due to the large non-linearity, high resistance to laser induced damage [6], low angular sensitivity and good mechanical hardness [7–9]. Among the semi organic non-linear optical materials, metal complexes of thiourea are applicable for high power frequency conversion [10]. Growth of bulk single crystals of these materials has been a subject of perennial concern to enable them to be useful for device applications. Some examples of semiorganic NLO materials are zin ctris (thiourea) sulphate (ZTS) [11-25], bis (thiourea) cadmium chloride (BTCC), zinc thiourea chloride (ZTC) and copper thiourea chloride (CTC). In the present work, the physical, structural, thermal, dielectric and piezo-electric, NLO properties of LMBTZS crystal was studied.

2. EXPERIMENTAL TECHNIQUES

2.1 Synthesis of NLO material

The thiourea and zinc sulphate was taken in 2:1 ratio.

$$2CS(NH_2)_2 + ZnSO_4 \rightarrow Zn[CS(NH_2)_2]_2SO_4$$

The thiourea and zinc sulphate was dissolved in distilled water and kept separately. The zinc sulphate solution was transferred into the thiourea solution. Immediately ZTS salt was precipitated in the solution then the product was separated and dried.

2.2 Growth of Single Crystal

The synthesized salt of ZTS was thoroughly dissolved in distilled water. Simultaneously 0.02 mol % of L-malic acid doped ZTS (LMBTZS) solution was prepared and allowed for crystallization. The grown crystals of size $0.8 \times 12 \times 0.5$ mm^3 were harvested in a period of 20 days (Fig. 1).

copyright © samriddhi, 2010-2019

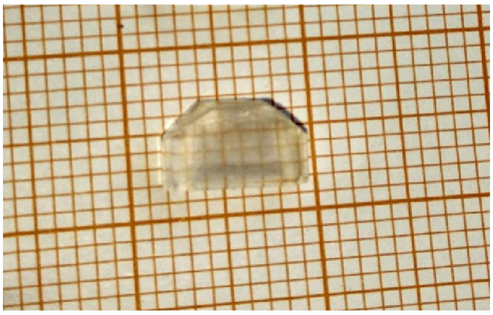

Fig.1: The as grown crystal of LMBTZS

3 RESULT AND DISCUSSION

3.1 FTIR Spectral Studies

The FTIR spectrum was recorded in the range of 4000 - 400 cm^{-1} (fig 2). The NH_2 symmetric stretching 3167 cm^{-1} in thiourea is shifted 3206 cm^{-1} in ZTS whereas in our sample it is shifted to 3186.4 cm^{-1}. The band at 3371.57cm^{-1} corresponds to asymmetric stretching vibration of NH_2 group. The N-H bending vibrations for primary amine of ZTS is at 1633 cm^{-1} whereas for LMBTZS it is shifted to 1635.64 cm^{-1}.The peak at 717.52 cm^{-1} and 1442.75 cm^{-1} shows the symmetric and asymmetric C=S stretching vibration respectively. The vibrations peak at 1033.85 cm^{-1} confirms the presence of sulphate ion. The observed frequencies and their assignment are listed in Table 1.

3.2 Force Constant

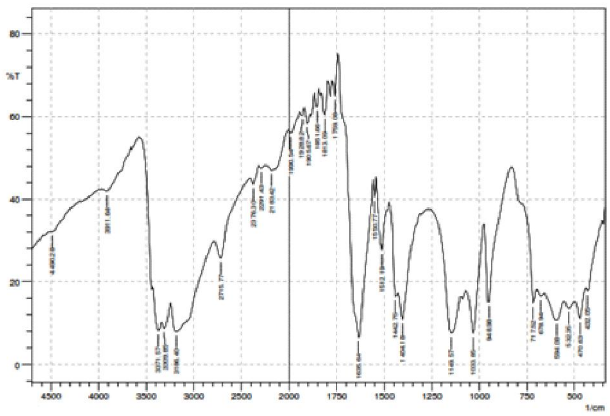

Fig.2: FTIR spectrum of LMBTZS crystal

Table-1: FTIR Assignments

THIOUREA	PURE ZTS	LMBTZS CRYSTAL	ASSIGNMENTS
411	424	432.05	$\delta_S(N-C-N)$
469	474	470.63	$\delta_S(C-S-N)$
740	717	717.52	$\vartheta_S(C=S)$
1089	1126	1033.85	$\vartheta_S(C-N)$
1417	1404	1442.75	$\vartheta_{as}(C=S)$
–	1515	1512.19	$\vartheta(N-C-N)$
1627	1633	1635.64	$\delta(NH_2)$
3167	3206	3186.4	$\vartheta_S(NH_2)$
3280	–	–	$\vartheta_S(NH_2)$
3376	3306	3371.57	$\vartheta_{as}(NH_2)$
–	3388	–	$\vartheta_{as}(NH_2)$

θ - Stretching, δ - bending, s - symmetric, as - asymmetric

The force constant, $K=4\pi^2V^2C^2\mu$ N/cm, of molecules are essential in the analysis of vibration spectra and are shown in Table 2.

Table-2

Force constant for C-N Stretching

C-N (WAVENUMBER cm^{-1})	FORCE CONSTANT K 10^5(N cm^{-1})
1032	4.05

Force constant for N-H_2 stretching

N-H_2 (WAVENUMBER cm^{-1})	FORCE CONSTANT K 10^5(N cm^{-1})
3184	10.4

Force constant for N-C-N stretching

N-C-N (WAVENUMBER cm^{-1})	FORCE CONSTANT K 10^5(N cm^{-1})
1507	11.2

3.2 Single Crystal XRD

The grown single crystal (LMBTZS) have been subjected to single crystal XRD using an ENRAFNONIOUS CAD - 4 automatic X-ray diffractometer with MoK$^{\alpha}$ radiations (λ=0.71073 Å) to determine the unit cell dimension (Table 3).

copyright © samriddhi, 2010-2019

The crystal system of LMBTZS belongs to orthorhombic. However due to doping of L-malic acid in BTZS there is remarkable change in the cell parameter of single crystal.

Table-3

Single crystal data for LMBTZS	
Wavelength	0.71073
Crystal system	Orthorhombic
Unit Cell Dimensions	
a=7.789(2) Å	α=90°
b=11.152(2) Å	β=90°
c=15.498(4) Å	γ=90°
Volume	1364.1(5) $Å^3$

3.3 Photoluminescence Spectral Studies

Photoluminescence (PL) is the process of emission of light when photons are excited from ground state. The photoluminescence spectrum of LMBTZS was recorded using Cary eclipse photoluminescence spectroscopy with an excitation wavelength of 380 nm (fig 3).

The spectrum shows that the strong emission of ultraviolet is observed at 388 nm corresponding

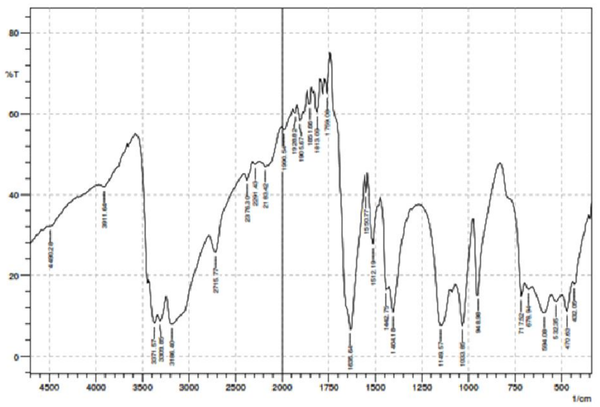

Fig.3: PL emissions of LMBTZS crystal

energy is 3.2 eV. The peak at 521 nm has the weak emission of green with energy of 2.38 eV. The peak at 780 nm has the weak emission of red light with energy of 1.59 eV, which is suitable for photonic device application. The band gap calculated in this work from PL study for LMBTZS found to be less than the band gap calculated for LMTTZS [32] in UV studies.

3.4 TG/DTA Analyses

The TG/DTA analysis of LMBTZS was carried out using thermal analyser SDT Q600 between 30-1100 °C in the nitrogen atmosphere (fig 4). The TG curve shows that the LMBTZS has good thermal stability upto 231.36 °C and the decomposition point found to be 248.83 °C. The sharpness of the melting curve indicates well crystalline of the sample. Since the thermal stability is high, it can be used in fabricating NLO devices.

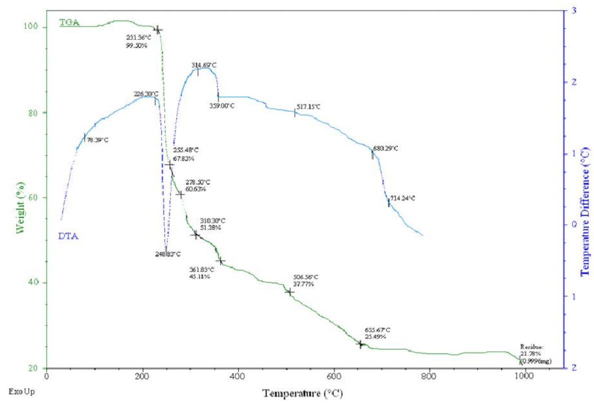

Fig.4: TG and DTA curves of the grown LMBTZS crystal

3.5 Piezo-electric Studies

The crystals were subjected to piezo-electric characterization using Ultrasonic Interferometer (for solids). The ultrasonic velocities are measured using the piezoelectric technique. Grease is found to be a good bonding medium to fix the transducer on the crystal sample surface and to admit these wave pulses into the sample. The presence of the bonding medium can introduce some additional phase change and because of the progressive

copyright © samriddhi, 2010-2019

decrease in the amplitude of the successive echoes, the judgment of the condition of the perfect overlap by visual evaluation also can introduce some error in the measured travel time.

The elastic properties of LMBTZS crystal were well studied by measuring ultrasonic velocity in the crystal in certain specified crystallographic directions and evaluating the elastic stiffness constants. Elastic constants are the only means to obtain information about the shear properties of the material. It provides information about the structural properties of the material. Furthermore, elastic moduli are sensitive indicators of certain phase transformations and provide information about the Inter atomic forces. At second order phase transformation, while many thermodynamic quantities show no obvious evidence of the transition, elastic constants may show discontinuities. One can use the discontinuities to learn about the phase transition. LMBTZS being an orthorhombic crystal has nine second order elastic stiffness constants. The elastic constants have direct relationship with the suitable ultrasonic mode velocity given by, $Cij = \rho v^2$ (Table 4). Thus the anisotropy in the elastic properties of the crystal can be studied.

Table-4: Measured mode Velocities of LMBTZS crystal at 308 K along different directions. Also relation between Elastic constants and mode Velocity.

SI.NO	MODE	MEASURED MODE VELOCITY (m/s)	MODE VELOCITY – ELASTIC CONSTANT RELATIONSHIP ($Cij = \rho v^2$)
1	L	1820	$3.30X10^6$
2	T	1810	$3.27X10^6$
3	QL	1790	$3.20X10^6$

L- LONGITUDINAL, T-TRANSVERSE, QL- QUASI LONGITUDINAL,

ρ - DENSITY OF THE SAMPLE (0.997×10^{-3} g/cc for LMBTZS crystal).

3.6 Dielectric Studies

Dielectric study of grown crystal was carried out in x-band at frequencies 8 kHz, 500 kHz, 1000 kHz at room temperature (309 K) using dielectric constant measuring kit. The dielectric constants of grown LMBTZS crystal via thiourea and zinc sulphate were determined.

It is observed that the dielectric constant decreases as frequency increases (fig 5). The ionic conductivity of crystal depends on the frequency of applied electric field. The dielectric constant depends on the amount of polarization when electric field is applied to polar material. At higher frequency there will be less polarization and dielectric constants decreases. The crystal with high dielectric constant lead to power dissipation. It is found that our grown sample LMBTZS has low dielectric constant.

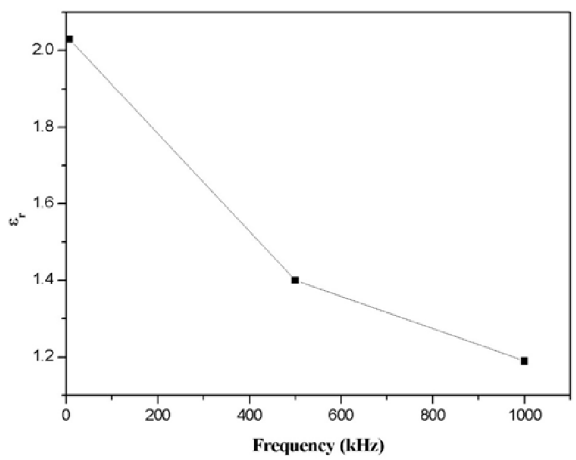

Fig.5: Variations of dielectric constant with frequency for LMBTZS crystal

The low values of dielectric loss at higher frequencies (fig 6) indicate that the grown crystal contains less defects and the samples are of good quality. The values of AC conductivity (fig. 7) are found to be increasing with increase of frequency. Variations of ln σ_{ac} versus frequency is shown in fig.8.

S-JPSET : Vol. 11, Issue 1, ISSN : 2229-7111 (Print) and ISSN : 2454-5767 (Online) copyright © samriddhi, 2010-2019

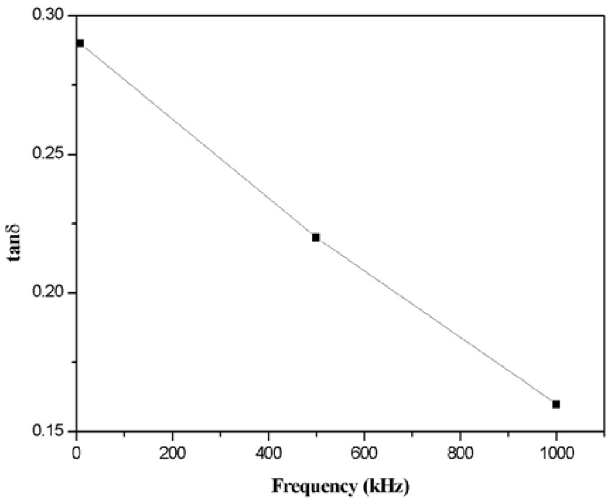

Fig.6: Variations of dielectric loss with frequency for LMBTZS crystal

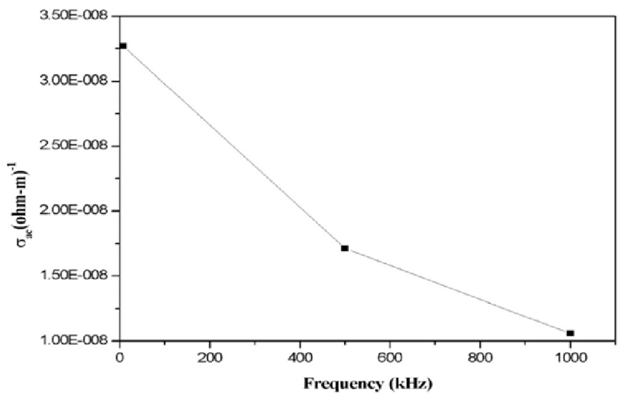

Fig.7: Variations of AC conductivity with frequency for LMBTZS crystal

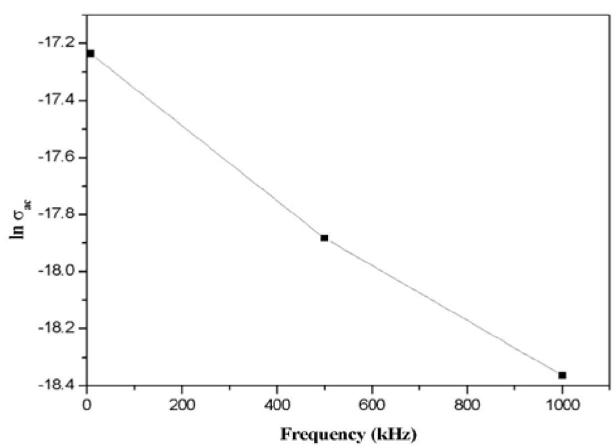

Fig.8: Variations of ln σ_{ac} versus frequency for LMBTZS crystal

3.7 Measurement of SHG Efficiency

The high intensity laser with the wavelength of 1064 nm was allowed to strike the sample using powder technique of Kurtz and Perry [26-32]. The SHG efficiency of LMBTZS is found to be 1.23 times that of KDP, confirmed by the emission of green radiation (532 nm) emitted by the sample.

4. CONCLUSION

The LMBTZS single crystals were grown by solution growth technique. The functional group of LMBTZS was confirmed by FT-IR analysis and the force constants were determined. The Single crystal XRD confirmed that LMBTZS crystals belong to orthorhombic system. The band gap calculated from PL study. TG/DTA curves shows that the sample is highly stable upto 231.36 ^{0}C LMBTZS is found to be an excellent piezo-electric material. The frequency study of LMBTZS crystal revealed that it has low dielectric constant compared to zinc sulphate and thiourea. Low dielectric constant of LMBTZS in comparison of its constituents makes it suitable for fabrication of high speed electro-optic modulators. The SHG efficiency of LMBTZS is found to be 1.23 times that of KDP

REFERENCES

[1] M. Diem, P.L. Polavarapu, M. Oboodi, L.A. Naûe, J. Am. Chem. Soc., 104 (1968) 1387.

[2] S.B. Monaco, L.E. Davis, S.P. Velsko, F.T. Wangand, D. Eimerl, J. Crystal Growth 85 (1987) 252.

[3] N. Zhang, M.H. Jiang, D.R. Yuan, D. Xu, X.T. Tao, Z.S. Shao, J. Crystal Growth 102 (1990) 581.

[4] U. Ramabadran, David E. Zelon, Gretchen C. Kennedy, Appl. Phys. Lett., 60 (1992) 2589.

[5] Z. Kotler, R. Hierle, D. Josse, J. Zyss, R. Masse, J. Opt. Soc. Am., B9 (1992) 534.

[6] N. Horiuchi, F. Lefaucheux, A. Ibanez, D. Josse, J. Zyss, Opt. Mater., 12 (1999) 351.

[7] M. Narayan Bhat, S.M. Dharmaprakash, J. Crystal Growth 236 (2002) 376.

[8] V. Venkataramanan, C.K. Subramanian, H.L. Bhat, J. Appl. Phys., 77 (1995) 6049.

[9] L.F. Warren, Eds. K.B Wischmann, Proceedings of the Fourth International Sample Electronics Conference, vol. 4, Society for the Advancement of Material and Process Engineering, Covina, CA (1990) 388.

[10] W.S. Wang, K. Sutter, Ch. Bosshard, Z. Pan, H. Arend, P. Gunter, G. Chapius, F.Nicolo, Jpn. J. Appl. Phys., 27 (1988) 1138.

[11] S. Moitra, T. Kar, Opt. Mats 30 (2007) 508.

[12] C. Krishnan, P. Selvarajan, S.Pari, Current Applied Physics 10 (2010) 664.

[13] Sweta Moitra, Tanusree Kar, Materials Chemistry and Physics 106 (2007) 8.

[14] J. Ramajothi, S. Dhanuskodi, and K. Nagarajan, Cryst. Res. Technol., 39 (2004) 414.

[15] N.R. Dhumane, S.S. Hussaini, V.V. Nawarkhele, and M.D. Shirsat, Cryst. Res. Technol., 41 (2006) 897.

[16] C. Krishnan, P. Selvarajan, T.H. Freeda, Materials Letters 62 (2008) 4414.

[17] M. Loganayaki, A. Senthil , P. Murugakoothan , International Journal of Computer Applications 72 (2013) 18-22.

[18] Sagadevan Suresh, American Chemical Science Journal 3, 3 (2013) 325.

[19] G.G. Muley, Journal of Electronic Materials 33 2 (2014) 1.

[20] S. Sudhahar, M. Krishna Kumar, B.M. Sornamurthy, R. Mohan Kumar, Spectrochimica Acta Part A: Molecular and Biomolecular spectroscopy, 118, 24 (2014) 929.

[21] Bincy Susan Samuel, R. Krishnamurthy, R. Rajasekaran, Spectrochimica Acta Part A: Molecular and Biomolecular Spectroscopy 132, 11 (2014) 526.

[22] Yachao Cao, Mingwei Li, Min Cheng, Jie Song, Zhitao Hu, J. Crystal Growth 388, 15 (2014) 22.

[23] M. Sumithra Devi, A.P. Arthi, K. Thamizharasan, Superlattices and Microstructures 73 (2014) 296.

[24] A. Kumaresh, R. Arun Kumar, M. Arivanandhan, Y. Hayakawa, J. Crystal Growth 401, 1 (2014) 874.

[25] T.C.Sabari GirisunandS.Dhanuskodi, Cryst. Res. Technol.,44 (2009)1297.

[26] S.S. Kurtz and T. Perry, J.Appl.Phys., 39 (1968) 3798.

[27] C. Krishnan, P. Selvarajan, Journal of Experimental Sciences1, 3 (2010) 23.

[28] C. Krishnan, P. Selvarajan, T.H. Freeda, Materials Letters 62 (2008) 4414.

[29] B.Sivasankari and P.Selvarajan, *International Journal of ChemTech Research* 7, 5 (2015) 2483.

[30] C. Krishnan, P. Selvarajan, S.Pari, Current Applied Physics 10 (2010) 664.

[31] B.Sivasankari and P.Selvarajan, Journal of Applied Science and Computations 5, 9 (2018).

[32] B.Sivasankari and P.Selvarajan, Optik127, 12, (2016) 4928.

 copyright © samriddhi, 2010-2019